The Effect of Impact Velocity Angle on Helmeted Head Impact Severity: A Rationale for Motorcycle Helmet Impact Test Design

Shiyang Meng, Madelen Fahlstedt, Peter Halldin

Abstract The impact velocity angle determined by the normal and tangential velocity has been shown to be an important description of head impact conditions but can vary in real-world accidents. The objective of this paper was to investigate the effect of impact velocity angle on helmeted head impact severity indicated by the brain tissue strain. The human body model coupled with a validated motorcycle helmet model was propelled at a constant resultant velocity but varying angle relative to a rigid surface. Different body angles, impact directions and helmet designs have also been incorporated in the simulation matrix (n=300).

The results show an influence of impact velocity angle on brain tissue strain response. By aggregating all simulation cases into different impact velocity angle groups, i.e., 15, 30, 45, 60 and 75 degrees, a 30- or 45-degree angle group give the highest median and inter-quartile range of the peak brain tissue strain. Comparisons of strain pattern and its peak value between individual cases give consistent results. The brain tissue strain is less sensitive to the body angle than to the velocity angle. The study suggests that UN/ECE 22.05 can be improved by increasing the current 'oblique' angle, i.e. 15 degrees inclined to vertical axis, to a level that can produce sufficient normal velocity component and hence angular head motion. This study also underline the importance of understanding post-impact head kinematics, and the need for further evaluation of human body models.

Keywords finite element method, head impact conditions, impact severity, motorcycle helmet, test method

I. INTRODUCTION

The head is one of the most frequently injured regions for powered two-wheeler (PTW) riders and is often found among moderate to severe injuries [1-4]. The main protection for the head is a motorcycle helmet, which is tested and certified today according to UN/ECE 22.05 [5], DOT FMVSS 218 [6] or SNELL M2015 [7] in Europe and US. In all existing test standards the helmets are dropped vertically to a flat or shaped surface. In addition, UN/ECE 22.05 includes a drop test onto an anvil inclined at 15 degrees to the vertical axis. This test method gives a high tangential velocity component (8.21 m/s) but low normal velocity component (2.20 m/s). The headform is however not instrumented to measure angular head motion, instead tangential force between helmet shell and the anvil is measured. More recently, Fédération Internationale de Motocyclisme (FIM) launched a Racing Homologation Programme (FRHP) [8] for helmets used in FIM competitions. Apart from the tests prescribed by the aforementioned international standards, the racing helmet is also dropped onto a 45 degrees anvil to create an equal tangential and normal velocity component (5.66 m/s). The question is if these test methods are the best possible way to certify a motorcycle helmet.

A helmet test standard shall be in a simplified and robust way to replicate common real-world accident situations [9] and be able to evaluate helmet protection performance [10]. This requires the basic understanding of real-world accidents and head impact biomechanics. The impact velocity angle determined by the normal and tangential velocity at a given impact location has been shown to be an important description of head impact conditions in real-world accidents [11-13]. However, the causal link between head impact conditions and impact severity is less understood.

Shiyang Meng (+39 334 7976536, shiyangm@kth.se) is a PhD student and Madelen Fahlstedt is a Post Doc Researcher in Biomechanics of Head and Neck Injuries, Peter Halldin is an Assistant Professor in Biomechanics of Head and Neck Injuries and Helmets at the Neuronic Engineering, School of Engineering Sciences in Chemistry, Biotechnology and Health, KTH Royal Institute of Technology, Stockholm, Sweden. Shiyang Meng is a R&D engineer at Helmet division of Dainese S.p.A., Italy.

Oblique impacts are more common than perpendicular impacts in motorcycling accidents [14-16]. When the rider is striking the ground in a single-PTW accident or after the collision with another vehicle, the impact velocity angle is determined by the rider's own horizontal velocity and vertical velocity. The COST 327 database [1] showed that head injuries occurred at a variety of body and head impact angles. Fifty percent of recorded head injuries occurred in shallow body impact angles (<15 degrees), and the second most frequent body impact angle is over 60 degrees. In addition, it has been found that the impact is mostly directed at the front and side of the head. Detailed head kinematics just before the impact can be extracted through accident reconstruction. Accident reconstructions using a multibody simulation approach [11-12] have shown that the impact velocity angle varied between 24 and 68 degrees as an acute angle between the impact velocity vector and tangential direction (or ground). Different impact velocity angles can give rise to varying normal velocity and tangential velocity component, which subsequently influence the inertial loading to the head. A previous study [17] has shown in three bicycle accident reconstructions that the influence on the brain tissue in form of brain tissue strain is more sensitive to tangential velocity compared to normal velocity.

Previous studies have shown the importance of the angular component in head impacts, which has also started to be introduced in motorcycle helmet test in the UN/ECE 22.05 and FIM's FRHP. Collection of accident data have shown that the body angle and impact velocity angle could vary a lot. The mentioned test standards use either a 15 degrees or 45 degrees angle at a similar impact speed, which is thought to be within the range of accident data. However, until now little is known how the different body angles and impact velocity angles are affecting the brain tissue. Therefore, the objective of this paper was to investigate the effect of impact velocity angle on helmeted head impact severity indicated by the brain tissue strain response of a human body model (HBM). This can be a consideration for helmet standards to test helmets at targeted impact severity levels, i.e., the worst-case scenario.

II. METHODS

Evaluation of Helmet Model with Experimental Oblique Impacts

The FE helmet model includes energy absorbing liner, outer shell, visor, spoiler, chin pad and chin strap, the mesh generation and material model is described in more detail in [21]. The FE model was previously compared with the linear impact tests for four impact locations and showed a difference in peak linear acceleration less than 5%. Further evaluation was made in this study with the oblique impact tests (Appendix 1). The comparison between experimental results and simulations are presented in Fig. 1, and the characteristics of acceleration responses are also analysed using CORA in Appendix 2. Overall, the FE helmet model correlated best with the experiments where the comfort liner was not included since the comfort liner has not been modelled due to numerical instabilities mentioned in [21]. The averaged CORA cross-correlation ratings for the experiments with comfort liner are 0.883 (linear acceleration) and 0.726 (angular acceleration), compared to 0.935 (linear acceleration) and 0.882 (angular acceleration) for the experiments without comfort liner. The difference in peak angular acceleration is 0.6-4.5% and 0.9-1.9% for peak angular velocity when compared with experiments without comfort liner. While the helmet model predicted well the peak linear acceleration (PLA) in linear impacts [21], i.e., less than 5% error, it gave relatively higher PLA in oblique impacts compared to the experiments, i.e., a difference of 10-19%. Reference [22] hypothesised that the combined shear and normal stresses, by having the tangential velocity component in addition to the normal velocity component, cause the foam to compress at a lower normal stress than for a perpendicular impact. Consequently, it reduces the peak headform force or linear acceleration as a result of the cracks developed in the foam. This may explain the difference in peak linear acceleration between the experiments and FE simulation as the current helmet model is limited to not modelling foam cracking and the weakening effect under combined shear and normal stresses. However, this can be considered as a conservative prediction from the current helmet model and its validity is sufficient for the purpose of this study.

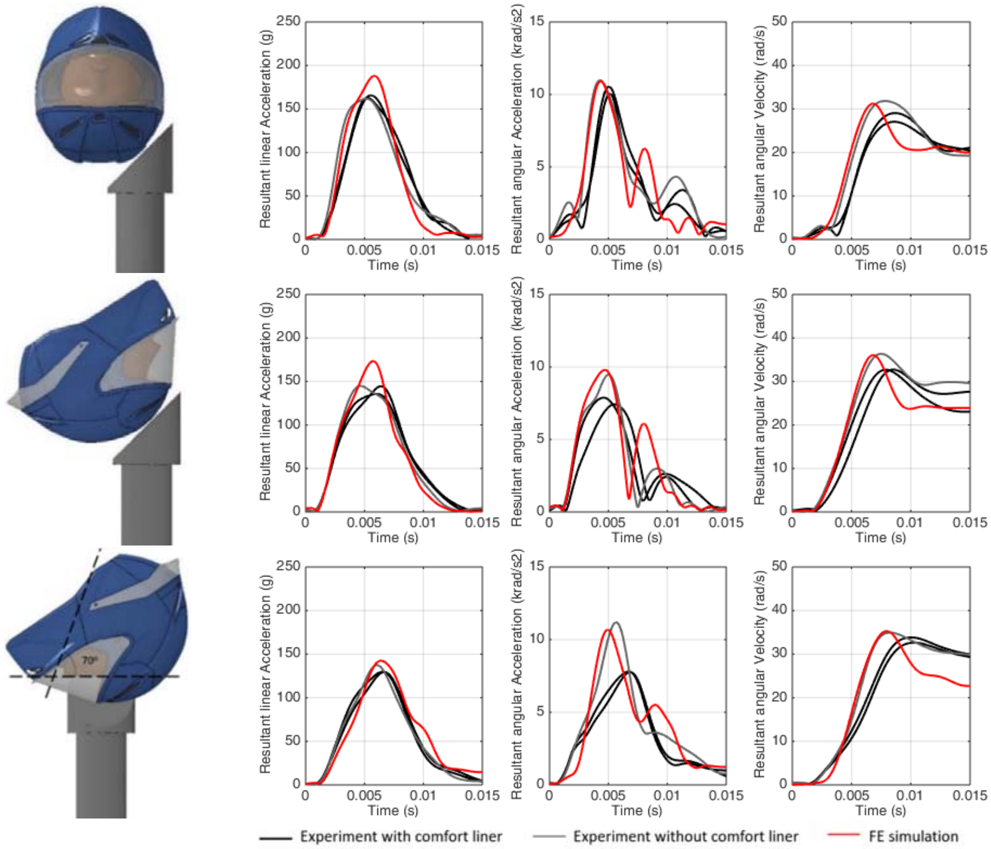

Fig. 1. Comparison of experimental oblique impact tests with FE simulations.

Helmeted HBM and Simulation Matrix

KTH head and neck model connected with Total Human Model for Safety (THUMS) Version 1.4 [18] [23-26], KTH-THUMS in short, was used in this study. The KTH head model has been validated against several relative motion experiments [27], localized brain motion, intracerebral acceleration and intracranial pressure experiments [28], and has previously been used in accident reconstructions [26][29]. The skull bone has been evaluated previously against impactor experiments in [17]. The scalp model used two-layered construction incorporating hyperplastic and viscoelastic behavior of the scalp [29]. The neck model used in this study has been previously validated at component level for flexion, extension, compression, lateral bending, axial rotation and tension [25] [30]. It has also been evaluated in dynamic compression against isolated head-spine complexes (i.e. no muscles) [30] in terms of head, neck forces and neck buckling mode. Furthermore, the model response was also compared with sled experiments on volunteers and Post Mortem Human Subjects (PMHS) for the head kinematics [24] [44].

A simulation matrix that propelled the HBM at a constant magnitude of the impact velocity vector, i.e., resultant velocity of 8.49 m/s, but varying impact velocity angle was designed, Fig. 2. In this way, the ratio between normal velocity component and tangential velocity component increased while raising the velocity angle (VA) from 15 to 75 degrees with 15-degree increment, Table I. Variations in body angle (BA), impact direction (Xrot, Yrot and Zrot) and helmet design (Helmet variation 1-5) were also included. Therefore, an acronym of Yrot_BA30_VA60 for example means that the impact direction is Yrot, body angle is 30 degrees and velocity angle is 60 degrees. The KTH head model is tilted slightly upwards and the inferior-superior axis of the head is 8 degrees to the longitudinal axis of the THUMS version 1.4. The five helmet variations are presented in Fig. 2. The coefficient of friction (cof) at the interface between helmet's interior and head was varied to 0.30 (helmet variation 2) and 0.15 (helmet variation 3) from the baseline helmet model (helmet variation 1) whose cof is 0.5. The baseline model was further modified into a soft helmet (helmet variation 4) and stiff helmet (helmet variation 5) by increasing or decreasing the energy absorbing liner density as well as the shell thickness, as shown in Table II. The performance of the baseline, soft and stiff helmet were evaluated virtually in accordance with UN/ECE 22.05, all three helmet variations met the 275g pass/fail criterion, i.e., 212g-274g. The change in stiffness altered not only the peak values but also the shape of the curve, Fig. 3. There are 60 simulations per helmet variation and therefore 300 simulations in total.

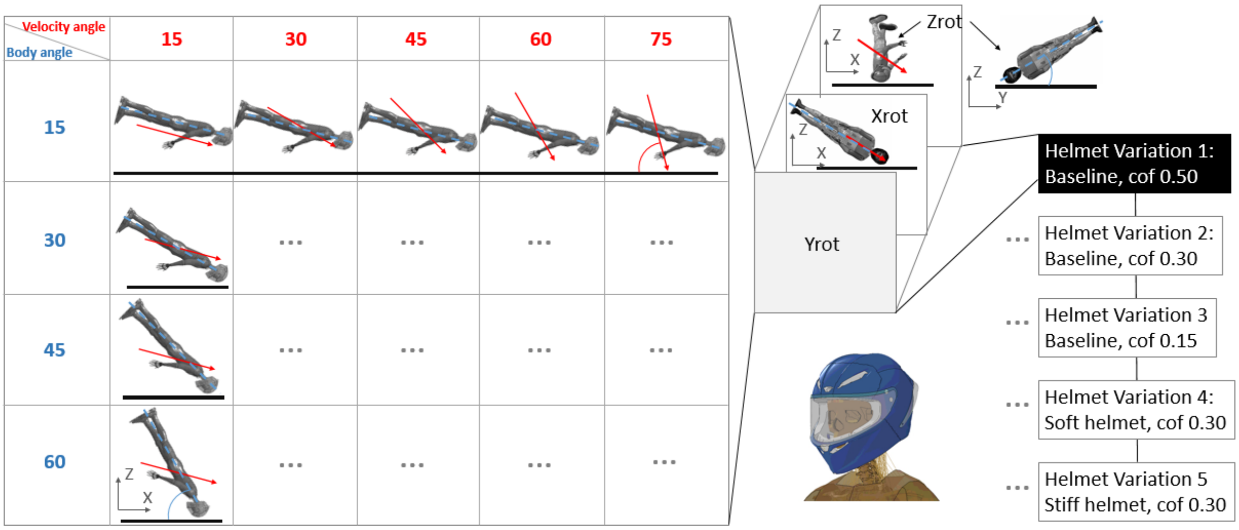

Fig. 2. The simulation matrix. Body angle was measured between the vertical axial of human body and impact surface, indicated by blue dashed line. The velocity angle is an acute angle between the velocity vector (red arrow) and impact surface. Xrot, Yrot and Zrot denote the three different impact directions.

TABLE I
VELOCITY IN TANGENTIAL AND NORMAL COMPONENT

	VA15°	VA30°	VA45°	VA60°	VA75°
Tangential (m/s)	8.21	7.36	6.01	4.25	2.20
Normal (m/s)	2.20	4.25	6.01	7.36	8.21
Ratio(N/T)	0.27	0.58	1.00	1.73	3.73

TABLE II
MODEL PARAMETERS FOR HELMET SOFT AND HELMET STIFF WITH REFERENCE TO BASELINE MODEL

	Baseline		Helmet Soft		Helmet Stiff	
	EPS density (kg/m^3)	Shell thickness (mm)	EPS density (kg/m^3)	Shell thickness (mm)	EPS density (kg/m^3)	Shell thickness (mm)
Front	75	2.0	65	0.7	80	2.0
Top	25	1.3	25	0.7	30	2.0
Side	55	1.3	45	0.7	60	1.3
Rear	45	1.3	45	0.7	45	2.0

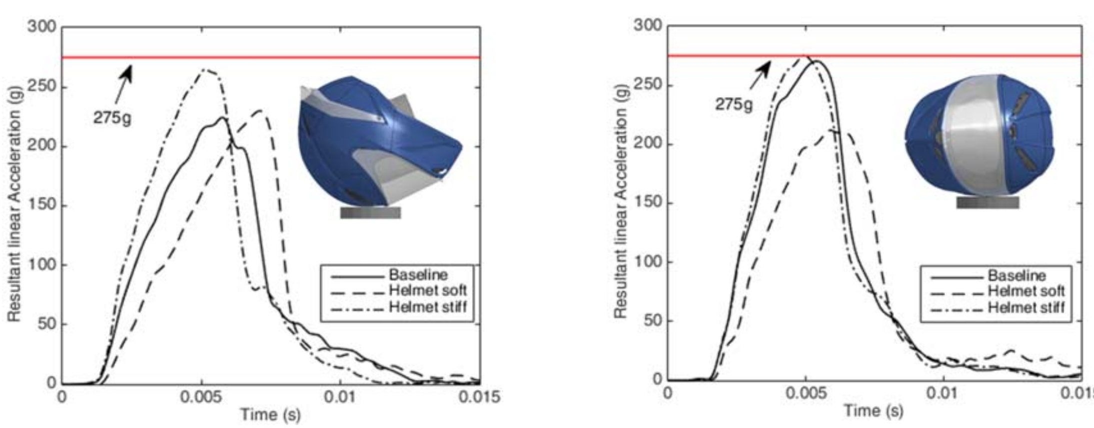

Fig. 3. The FE helmet models coupled with an EN960 headform was dropped at 7.5 m/s against a flat anvil of 130 mm diameter at front (left) and side (right).

The impact surface was modelled as rigid. The coefficient of friction at the interface between the ground and helmet was set to 0.5. All simulations were performed using the software LS-DYNA (v971 R7.1.2, smp, single precision; LSTC, Livermore, CA, USA). Analysis of the results was performed with LS-PrePost (version 3.2, LSTC, Livermore, CA, USA) and Matlab (version R2014b, The MathWorks Inc, Natrick, MA, US). The simulations were analysed from when the magnitude of linear acceleration exceeded 3g until the major component of linear acceleration (the one with the highest peak linear acceleration magnitude) returned zero. If the linear acceleration did not return to zero, a threshold of 4g was searched to determine the end time instead. A similar approach has been used previously in experimental testing of various types of motorcycle helmet [31]. Both the six degree-of-freedom head kinematics and the first principal Green-Lagrange strain of the whole brain were extracted from simulations. As Brain Injury Criterion (BrIC) [32] is implemented as an acceptance criterion in FIM FRHP, BrIC was also computed for each simulation.

III. RESULTS

The mean duration of the impulse in the helmeted head impact was ranged from 11.1 ms (stiff helmet) to 14.5 ms (soft helmet). However, it was found that the duration differed depending on specific impact configuration, i.e., velocity angle, impact direction and body angle, which is exemplified in Fig. 4.

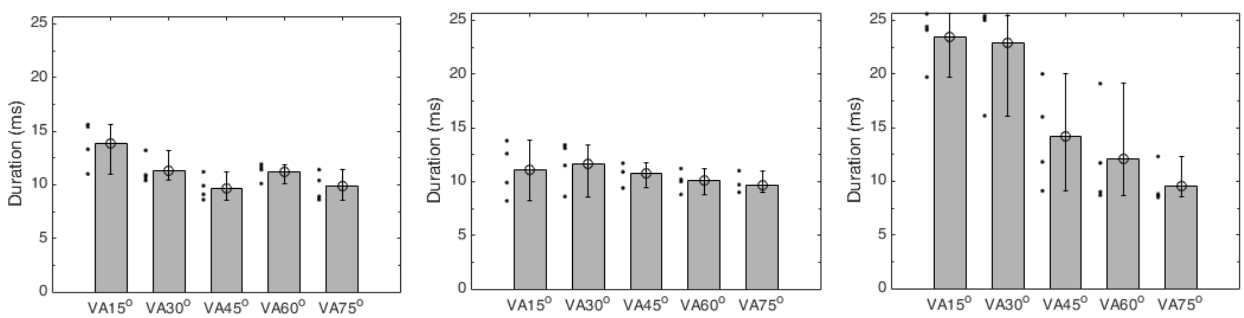

Fig. 4. Head impact duration of helmet variation 2 (cof 0.3) for Xrot (left), Yrot (middle) and Zrot (right). The column denotes the mean duration calculated from four body angles with the error bar of each column showing the range. The small black dots are data points.

Fig. 5 provides an overview of the peak first principal Green-Lagrange (G-L) strain for all the simulations and compares groups of data, i.e., velocity angles (VA) and body angles (BA) in the three impact directions. A curvilinear pattern was identified for the velocity groups with VA30 or VA45 being the highest among the others, which is indicated by the median and inter-quartile range (IQR) of the strain. For body angle, the difference in median and IQR between different body angle groups is less than that of the velocity angle groups. In addition, the data spread (minimum to maximum) and the IQR are generally higher than that of the velocity angle groups, which suggests higher data variation in each body angle group. Furthermore, it is shown that the strain in the impact direction Xrot was generally lower than that in Yrot and Zrot. The outlier plotted as asterisk in Fig. 5 is a data point that falls more than 1.5 times the IQR above the third quartile or below the first quartile. There are five cases/outliers in the velocity angle groups (Xrot_BA30_VA75 and Xrot_BA60_VA75 of helmet variation 1, Zrot_BA60_VA60 of helmet variation 5, Zrot_BA15_VA30 and Zrot_BA30_VA30 of helmet variation 3) and one case (Xrot_BA15_VA30 of helmet variation 1) in the body angle groups.

Fig. 6 shows resultant linear and angular acceleration, angular velocity and brain tissue strain with varied velocity angles for the Zrot_BA15 simulations of helmet variation 2. It is shown that with increasing velocity angle, which give a higher normal velocity component, the peak linear acceleration increases. However, the same is not true for peak angular acceleration and peak change in angular velocity. The level of peak angular velocity mirrored that of the peak brain tissue strain. Fig. 7 illustrated how the tissue strain patterns changed with the impact conditions, from some representative cases. There is strain enhancement and enlarged area of higher level of strain at VA30 and VA45 regardless of impact directions. The prominent areas of higher strain involved cerebral cortex, sub-cortex as well as some deep brain structures. These areas has not been varied distinctively with different impact velocity angles but with different impact directions.

Fig. 8 shows heat maps consisting of all 300 simulation cases arranged by the five helmet variations (in the row) and the three impact directions (in the column). Each heat map tabulated numeric value of peak first principal Green-Lagrange strain along with the grayscale indicating the strain level for each simulation case. Velocity angles (VA) and body angles (BA) are in the X- and Y-axis of the heat map, respectively. In general, as shown in Fig. 8, the level of strain was in a graded fashion over different velocity angles and higher strain levels were clustered around VA30 and VA45, and this cluster of higher strain persisted for different helmet variations. The worst-case scenario can be identified by the highest strain value per helmet variation. The highest BrIC values were concentrated at VA30 or VA45 (Fig. C1, Appendix 3), which followed the same trend as for peak brain tissue strain (Fig. 8). Moreover, the worst case determined by the level of BrIC vaule specifically at each impact direction correlates with that determined from peak brain strain.

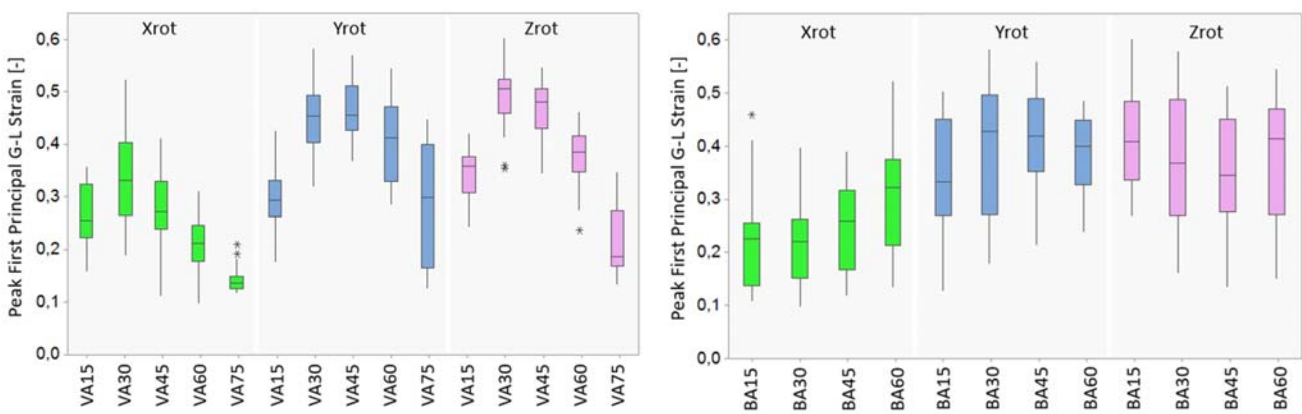

Fig. 5. Box plot. The strain data of all simulations (n=300) are divided into groups based on velocity angles (left) and on body angles (right), for three different impact directions. Twenty and twenty-five data points are for each group of velocity angle and body angle, respectively.

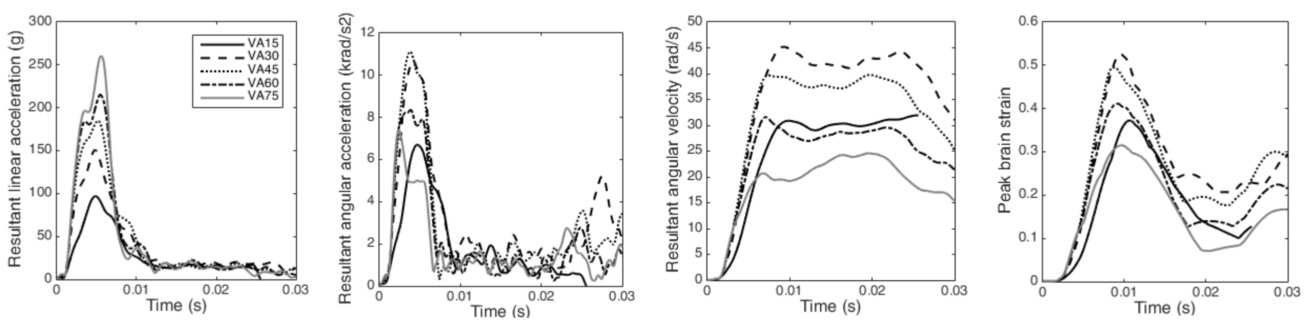

Fig. 6. Curves for Zrot_BA15 (helmet variation 2) exemplify head kinematics and brain tissue strain at different impact velocity angles.

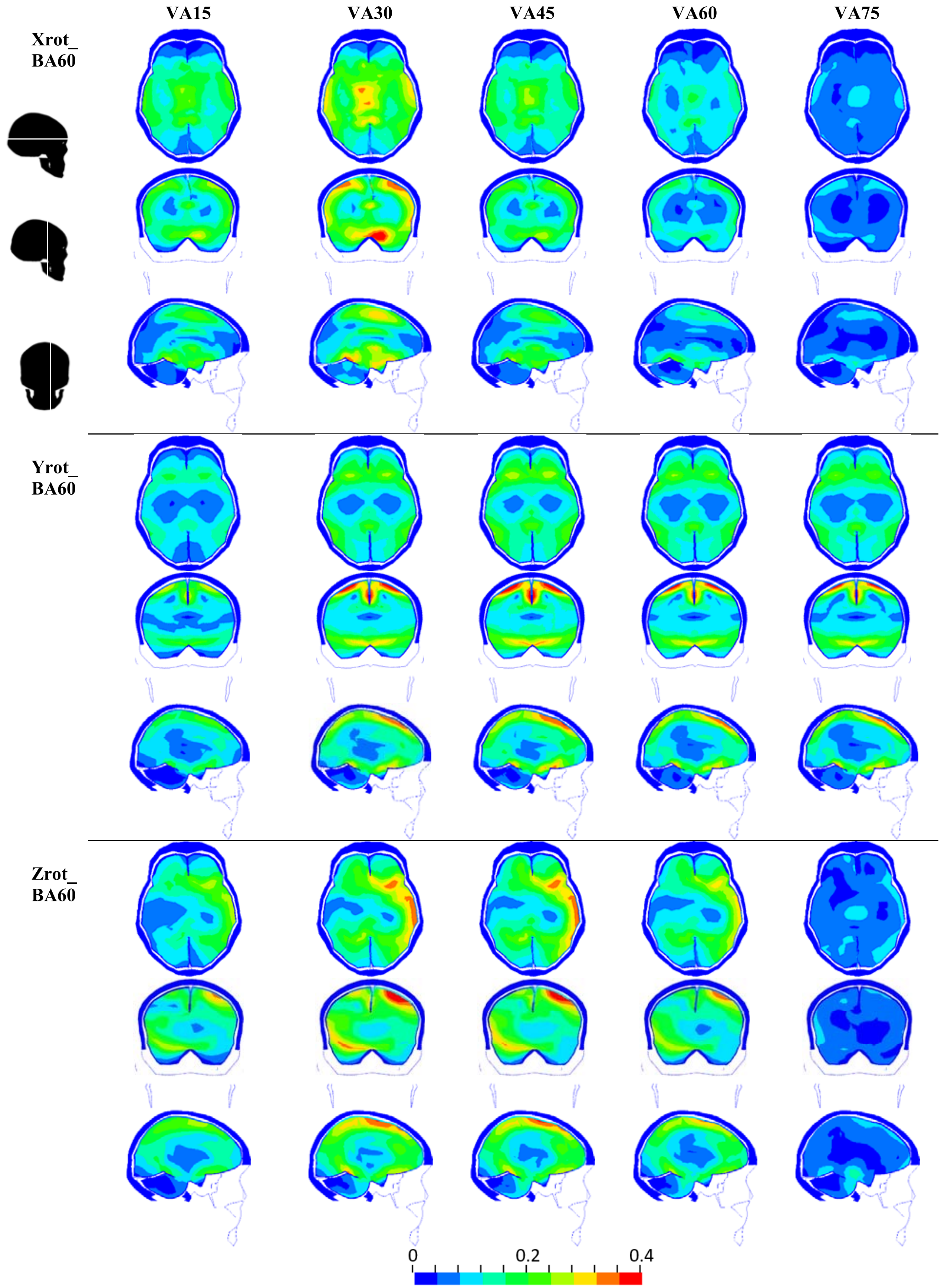

Fig. 7. Tissue strain pattern at the maximum occurring time over different impact velocity angles for simulation cases of helmet variation 2.

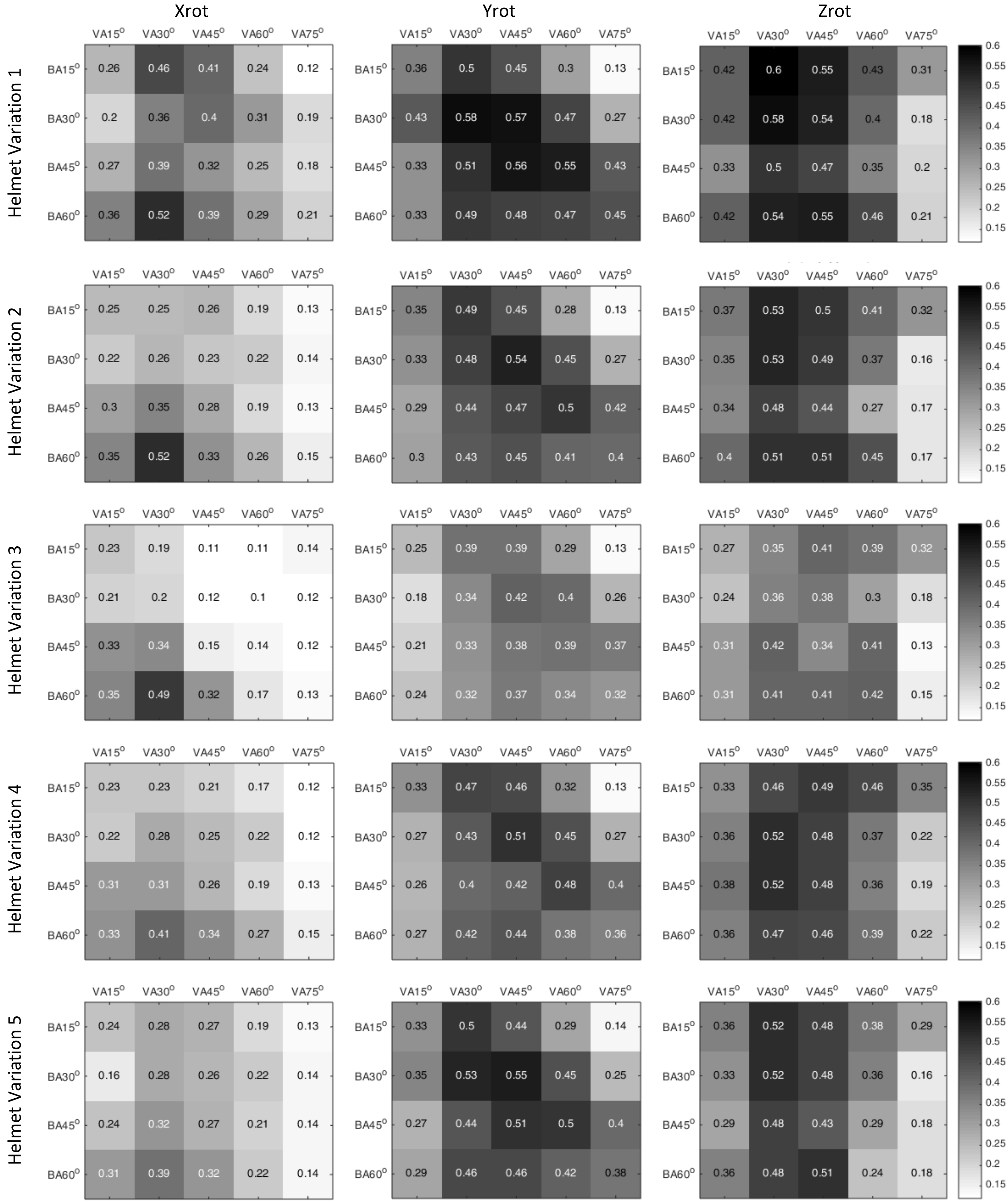

Fig. 8. Heat map shows the numerical value along the colour scale indicating the level of peak brain strain developed during the helmeted head impact for the entire simulation matrix. Body angle (BA) and velocity angle (VA) are variables along the two axes, the simulation results are arranged by helmet variation in the row and impact direction in the column. The darker colour indicates higher strain, and vice versa.

IV. Discussion

This paper investigates the effect of impact velocity angle and body angle on helmeted head impact severity in order to enhance our understanding of the causal link between head impact condition and impact severity. An overall display of data (peak first principal G-L strain) that grouped into different velocity angles (VA15, VA30, VA45, VA60 and VA75) has shown that the median and IQR are highest in the VA30 or VA45 group, Fig. 5. Less difference in median and IQR between different body angle groups (BA15, BA30, BA45 and BA60) suggests that the peak brain tissue strain is less sensitive to the body angle than to the velocity angle. On a case-by-case comparison, it is shown in Fig. 8 that a clustering of high peak strain values are around VA30 and VA45, which reinforces the observation made from the grouped data. In addition, tissue strain patterns in Fig. 7 indicate strain enhancement and enlarged area of higher level of strain at VA30 and VA45, which is consistent with the above findings.

Previous studies [11-12] showed that the head impact velocity vector, which is described by both magnitude (resultant velocity) and direction (impact velocity angle), can vary in real-world motorcycle accidents. As both can contribute to the severity of head impact, this study isolated the magnitude as a control to avoid complication. Given the constant resultant velocity, i.e., 8.49 m/s, the ratio between normal and tangential velocity component increases with the impact velocity angle. References [22][33] showed that the increase of the peak headform force is a nearly linear function of the velocity in a linear impact, and that the linear acceleration is not significantly altered by the tangential velocity component in an oblique impact. This is due to the peak deformation of energy absorbing liner increasing almost linearly with normal velocity [34]. In this paper, as the impact velocity angle increases (so as the normal velocity component), the linear acceleration increases as well. However, the relationship between the impact velocity angle and angular acceleration pulse is more complex. Angular acceleration can be contributed by both the friction at sliding interfaces and the moment generated by a normal force offset to the centre-of-gravity (COG) of the head. Therefore, a shallow impact velocity angle, i.e., 15 degrees, has a lower normal velocity component (2.2 m/s), resulting in a lower normal force (F_n). As the tangential force (F_t) causing the rotational kinematics is related to the normal force by the relationship $F_t=\mu*F_n$ where μ is the coefficient of friction, a reduced normal force will cause less tangential force and then possibly less angular head motion. A previous study [35] used FE simulations of oblique impact tests involving a Hybrid III head-only and the impact velocity angle was varied (30, 45, 60 and 90 degrees) at different impact speed (5, 7 and 9m/s). The results showed that the 30 degrees angle produced the highest angular velocity at each impact speed tested. Another study [36], testing bicycle helmets for preadolescents also discovered that a 30-60 degrees anvil appeared to be a good tradeoff between rotational and translational loading. This paper confirms the above findings resulted from a laboratory model of oblique impacts and gives direct causal relationship between impact condition and brain tissue strain from a HBM.

References [28][37] found that the influence of impact direction had a substantial effect on the intracranial response, and that the change in angular velocity corresponded best with the intracranial strains found in the FE head model when subjected to an impulse with varied duration up to 20 ms. This finding is in agreement with Holbourn's hypothesis that the injury is proportional to the change in angular velocity for rotational impulses of short durations via observing shear strain patterns in 2D gel models, as well as in agreement with an analytical model of traumatic diffuse brain injury [38-39]. The BrIC formulation that comes from a more recent publication [32] takes angular velocity and impact direction into account. Therefore, it is not surprising to see in Fig. C1 that a similar trend of impact severity is achieved via BrIC as compared with the peak brain tissue strain. It is also worth to mention that the loading generated from the impact directions of this study (i.e. Xrot, Yrot and Zrot) involves impulses around all three local head axes with different levels, hence it is not equivalent to and shall not be inferred to the head injury tolerance in different directions which is normally implied by a constant impulse for different directions.

The helmet shell and road friction coefficient, thereby the *sliding resistance*, is not the only factor determining the headform rotational motion [13][16][40-41]. A mass, spring and damper model of the helmet also indicates that the force acting on the helmet outer shell is not necessarily that experienced by the head [33]. The present simulation matrix consists of the three coefficients of friction (0.5, 0.3 and 0.15) between the head and the helmet interior, and it has shown that the interior friction had an effect on the head kinematics and resulting brain tissue strain. The results of this study can add to the previous suggestion that angular head motion should be measured directly at headform's COG for oblique impact and linear impact in ECE22.05 [21][41]. Furthermore, UN/ECE 22.05 have a 15-degree anvil reproducing oblique impact with an impact velocity angle of 15 degrees at speed of 8.5 m/s, which would according to the results presented in this study not represent some of the severe or worst case scenarios. An improvement would be either to increase the angle of the impact anvil or to raise the drop speed in order to give a higher normal velocity component. However, the drop speed has often been constrained by the available roof height of testing laboratories in practice.

There are a number of limitations in this study. First, the results are based on the simulations of a HBM, which may be limited by the limitations of the model itself. The previous neck model validations have been limited to the available experiments found in the literature, and has intended primarily on providing a realistic boundary condition for the head such that the head kinematics is captured upon inertial loading and direct impact. The current study includes extensive loading conditions that would require extended neck validation. The flesh surrounding the neck could also be included to provide some constraints on the range of motion and to avoid unrealistic contact between chin and vertebral bodies in some cases. The model in current study only used passive muscle properties, previous study [18] demonstrated that muscle activation is another important consideration. Recent experiment on scalp-skull sliding using cadaver heads [45] may also provide data for further evaluation of the sliding behavior of the scalp. Secondly, for the helmet design it is only the stiffness and interaction between the helmet and head that has been varied but not the helmet geometry, which could influence the results, especially as the initial contact point would differ when altering the body impact angles. Third, the simulation matrix could be further expanded by considering different combinations of head angle (i.e. chin up or down) and body angle. Fourth, the fidelity of post-impact head kinematics have not been studied in detail in the past. The results presented above is limited to 10-25 ms based on the duration of the linear acceleration. However, the head kinematics could be further affected by the interaction between the body and ground, which could influence the brain tissue strain in the model. To illustrate this, a few cases of the whole-body (WB) simulations are compared with head-only (HO) simulations for 30 ms (Appendix 4). Fig. D1 shows an example (Zrot_BA45_VA45) where the HO simulation have made relatively small difference to the WB kinematics and strain. However, Xrot_BA15_VA45 and Yrot_BA45_VA45 show another example with dissimilar angular kinematics between HO and WB. The main component of angular velocity of HO simulations plateau at a time that is less than 15 ms and then gradually decay toward zero whereas the WB simulations tend to decay more drastically and eventually reverse direction. This reversal of angular velocity direction may have caused two consecutive peak of brain strains with the second peak relatively higher than the first peak. In the Xrot case the shoulder interacts with the ground, and alters the rotation of the head, which gives different head kinematics compared to the HO case. In the Yrot case, the chin interacts with the vertebral column directly since the flesh and muscles is not modelled with solid elements. As the second peak occurs after the helmeted impact, it can be postulated that the boundary conditions of the head become a more dominant contributor rather than the helmet itself. However, this is just speculation and the human body models need further evaluations before further conclusions can be made on how this could affect the helmet design and future helmet test methods. The implication of post-impact head kinematics for a helmet test method is not trivial and therefore need further investigation. Lastly, this study has focus on the influence on the brain tissue. The change in prescribed impact condition in this study could also influence the global loading modes on the vertebral column and subsequently affect the outcome of neck injuries as well, which is not evaluated in this study.

V. CONCLUSIONS

This study has shown that for five different helmet designs with different head-helmet interaction and helmet stiffness, the impact velocity angle of 30-45 degrees is the most severe for the peak brain tissue strain measured in the KTH FE head model and BrIC. The main reason for the results is that the normal force needs to be of a certain level compared to the tangential force to drive the angular velocity that is correlating to the strain in the brain.

VI. ACKNOWLEDGEMENT

This work was supported by the European Union Horizon 2020 Research and Innovation Programme under the Marie Skodowska-Curie Grant Agreement No. 642662. The acknowledgment is extended to Svein Kleiven and Alessandro Cernicchi for helpful suggestions on the manuscript. The authors would also like to acknowledge MIPS AB for the use of the helmet testing facility and Dainese S.p.A. for providing helmets and continuous support.

VII. REFERENCES

[1] Chinn B, Canaple B, et al. COST 327 Motorcycle safety helmets. European Commission, Directorate General for Energy and Transport, 2001.

[2] MAIDS, A. In-depth investigation of accidents involving powered two-wheelers. Final report 1.2. Brussels: Association of European Motorcycle Manufacturers (ACEM), 2004.

[3] Piantini, S., Pierini, M., et al. Injury Analysis of Powered Two‐Wheeler versus Other‐Vehicle Urban Accidents. *Proceedings of IRCOBI Conference,* 2016, Malaga, Spain.

[4] Otte, D., Chinn, B., Doyle, D., Sturrock, K., and Schuller, E. Interim Report Database COST 327 Accident Description and Analysis of Motorcycle Safety Helmets. Medical University Hannover, Germany, 1998.

[5] UNECE Regulation. Uniform provisions concerning the approval of protective helmets and their visors for drivers and passengers of motorcycles and mopeds (UN ECE 22.05). 2002: Geneva.

[6] Federal Motor Vehicle Safety Standard. Motorcycle Helmets (FMVSS 218). 2011: Washington, DC.

[7] Snell Memorial Foundation. Standard For Protective Headgear For Use with Motorcycles and Other Motorized Vehicles (SNELL M2015). 2015.

[8] FIM. FIM Racing Homologation Programme for Helmets. 2017: Mies, Switzerland.

[9] Halldin, P Kleiven, S. The development of next generation test standards for helmets. *Proceedings of the 1st International Conference on Helmet Performance and Design*, 2013, London, UK.

[10] McIntosh, A.S., Andersen, T.E., et al. Sports helmets now and in the future. *British Journal of Sports Medicine*, 2011. 45(16): p. 1258-1265.

[11] Bourdet, N., Deck, C., Tinard, V., and Willinger, R.m. Behaviour of helmets during head impact in real accident cases of motorcyclists. *International Journal of Crashworthiness*, 2012. 17(1): p. 51-61

[12] Bourdet, N., Mojumder, S., et al. Proposal of a new motorcycle helmet test method for tangential impact. *Proceedings of IRCOBI Conference,* 2016, Malaga, Spain.

[13] Ebrahimi, I., Golnaraghi, F., and Wang, G.G. Factors influencing the oblique impact test of motorcycle helmets. *Traffic injury prevention*, 2015. 16(4): p. 404-408.

[14] Aldman, B., Lundell, B., and Thorngren, L. Oblique impacts-a parametric study in crash helmets. *Proceedings of IRCOBI Conference*, 1978, Lyon, France.

[15] Aldman, B., Lundell, B., Thorngren, L., and Turbell, T. Helmet attenuation of the head response in oblique impacts to the ground. *Proceedings of IRCOBI Conference,* 1978, Lyon, France.

[16] Aare, M. and Halldin, P. A new laboratory rig for evaluating helmets subject to oblique impacts. *Traffic injury prevention*, 2003. 4(3): p. 240-248.

[17] Fahlstedt, M., Baeck, K., et al. Influence of impact velocity and angle in a detailed reconstruction of a bicycle accident. *Proceedings of IRCOBI Conference*, 2012, Dublin, Ireland.

[18] Fahlstedt, M., Halldin, P., S Alvarez, V., and Kleiven, S. Influence of the Body and Neck on Head Kinematics and Brain Injury Risk in Bicycle Accident Situations. *Proceedings of IRCOBI Conference*, 2016, Malaga, Spain.

[19] Feist, F. and Klug, C. A Numerical Study on the Influence of the Upper Body and Neck on Head Kinematics in Tangential Bicycle Helmet Impact. *Proceedings of IRCOBI Conference,* 2016, Malaga, Spain.

[20] Ghajari, M., Galvanetto, U., Iannucci, L., and Willinger, R. Influence of the body on the response of the helmeted head during impact. *International journal of crashworthiness*, 2011. 16(3): p. 285-295.

[21] Meng, S., Cernicchi, A., Kleiven, S., and Halldin, P. The Biomechanical Differences of Shock Absorption Test Methods in the US and European Helmet Standards. *International journal of crashworthiness*, https://doi.org/10.1080/13588265.2018.1464545.

[22] Mills, N. and Gilchrist, A. Response of helmets in direct and oblique impacts. *International journal of crashworthiness*, 1996. 2(1): p. 7-24.

[23] Alvarez, V.S., Fahlstedt, M., Halldin, P., and Kleiven, S. Importance of neck muscle tonus in head kinematics during pedestrian accidents. *Proceedings of IRCOBI Conference*, 2013, Gothenburg, Sweden.

[24] Alvarez, V.S., Halldin, P., and Kleiven, S. The influence of neck muscle tonus and posture on brain tissue strain in pedestrian head impacts. *Stapp Car Crash Journal*, 2014. 58: p. 63-101.

[25] Brolin, K. and Halldin, P. Development of a finite element model of the upper cervical spine and a parameter study of ligament characteristics. *Spine*, 2004. 29(4): p. 376-385.

[26] Kleiven, S. Predictors for traumatic brain injuries evaluated through accident reconstructions. *Stapp Car Crash Journal*, 2007. 51: p. 81-114.

[27] Kleiven, S. and Hardy, W.N. Correlation of an FE model of the human head with local brain motion: Consequences for injury prediction. *Stapp Car Crash Journal*, 2002. 46: p. 123-144.

[28] Kleiven, S. Evaluation of head injury criteria using a finite element model validated against experiments on localized brain motion, intracerebral acceleration, and intracranial pressure. *International Journal of Crashworthiness*, 2006. 11(1): p. 65-79.

[29] Fahlstedt, M., Depreitere, B., Halldin, P., Vander Sloten, J., and Kleiven, S. Correlation between injury pattern and finite element analysis in biomechanical reconstructions of traumatic brain injuries. *Journal of biomechanics*, 2015. 48(7): p. 1331-1335.

[30] Halldin, P., Brolin, K., Kleiven, S., Jakobsson, L., and Palmertz, C. Investigation of conditions that affect neck compression-flexion injuries using numerical techniques. *Stapp Car Crash Journal*, 2000. 44: p. 127-138.

[31] Lloyd, J. Biomechanical Evaluation of Motorcycle Helmets: Protection against Head and Brain Injuries. *Journal of Forensic Biomechanics*, 2017. 8(135): p. 2.

[32] Takhounts, E.G., Craig, M.J., Moorhouse, K., McFadden, J., and Hasija, V. Development of brain injury criteria (BrIC). *Stapp car crash journal*, 2013. 57: p. 243-266.

[33] Gilchrist, A. and Mills, N. Modelling of the impact response of motorcycle helmets. *International journal of impact engineering*, 1994. 15(3): p. 201-218.

[34] Mills, N., "Polymer foams handbook: engineering and biomechanics applications and design guide". 2007: Elsevier.

[35] Aare, M., Kleiven, S., and Halldin, P. Injury tolerances for oblique impact helmet testing. *International journal of crashworthiness*, 2004. 9(1): p. 15-23.

[36] Klug, C., Feist, F., and Tomasch, E. Testing of bicycle helmets for preadolescents. *Proceedings of IRCOBI Conference*, 2015, Lyon, France.

[37] Kleiven, S. Influence of impact direction on the human head in prediction of subdural hematoma. *Journal of neurotrauma*, 2003. 20(4): p. 365-379.

[38] Margulies, S.S. and Thibault, L.E. An analytical model of traumatic diffuse brain injury. *Journal of biomechanical engineering*, 1989. 111(3): p. 241-249.

[39] Margulies, S.S. and Thibault, L.E. A proposed tolerance criterion for diffuse axonal injury in man. *Journal of biomechanics*, 1992. 25(8): p. 917-923.

[40] Finan, J.D., Nightingale, R.W., and Myers, B.S. The influence of reduced friction on head injury metrics in helmeted head impacts. *Traffic injury prevention*, 2008. 9(5): p. 483-488.

[41] Mills, N. Critical evaluation of the SHARP motorcycle helmet rating. *International journal of crashworthiness*, 2010. 15(3): p. 331-342.

[42] Padgaonkar, A.J., Krieger, K., and King, A. Measurement of angular acceleration of a rigid body using linear accelerometers. *Journal of Applied Mechanics*, 1975. 42(3): p. 552-556.

[43] Gehre, C., Gades, H., and Wernicke, P. Objective rating of signals using test and simulation responses. *Proceedings of International Technical Conference on the Enhanced Safety of Vehicles*, 2009.

[44] K. Brolin, P. Halldin, and I. Leijonhufvud, The Effect of Muscle Activation on Neck Response, *Traffic Injury Prevention,* 2005, p. 67–76.

[45] Trotta, A., et al. Evaluation of the head-helmet sliding properties in an impact test. *Journal of Biomechanics*, https://doi.org/ 10.1016/j.jbiomech.2018.05.003, 2018.

[46] PDB (Partnership for dummy technology and biomechanics), CORA Release 3.6 User’s Manual. Available at http://www.pdb-org.com/en/information/ 18-cora-download.html.

VIII. APPENDIX

Appendix 1 – Helmet Experimental Tests

The helmets (AGV Pista GP) that coupled with the Hybrid III 50th percentile headform were dropped at 7.5 m/s onto a 45 degrees anvil covered with abrasive paper (i.e. 40 grit sandpaper). Consistent helmet fitting was ensured by measuring the distance between Hybrid III nose and front edge of helmet, which is about 7cm. There are three impact configurations, namely Impact1, Impact2 and Impact3, Fig. A1. For Impact1 and Impact2, the helmeted head was positioned such that the (skull) base of the headform was horizontal. The skull base is 70 degrees to horizontal for Impact3. The headform was instrumented with nine accelerometers in a 3-2-2-2 array at its COG, which allows acquisition of both linear and angular accelerations [42]. The data was filtered with a SAE 180 filter before it was analysed.

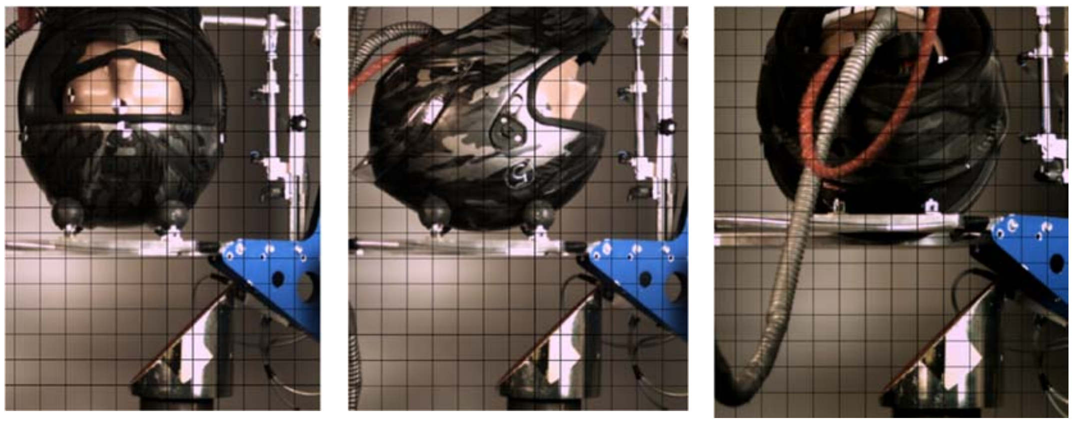

Fig. A1. Test configurations from left to right: Impact1, Impact2 and Impact3.

Appendix 2– Helmet Model CORrelation and Analysis (CORA)

To perform a quantitative comparison of response characteristics between experimental results and simulations, cross-correlation analysis was carried out using CORA v3.6. The analysis is based on curve shape (cross correlation function), size and phase shift. A single score is then calculated for the correlation method by taking a weighted sum of all three metrics. The rating from 0 and 1 denotes a match between unacceptable and excellent.

Recommended global settings for cross-correlation methods from CORA user's manual [46] were adopted in this analysis. The start (time) and end (time) of the interval of evaluation were manually set between 0 and 25 ms, which covers the whole impact pulse. The correlations were based on the resultant acceleration curves. The comparison was performed for both tests with and without the comfort liner. For two repeated experiments, the correlation analysis was performed with each individual curve and then averaged to provide a single score.

TABLE AI
COMPARISON BETWEEN EXPERIMENTS AND SIMULATIONS FOR LINEAR AND ANGULAR ACCELERATION RESPONSES

		CORA	Rating (Lin. Acc.)	Rating (Ang. Acc.)
Impact1	With comfort liner	Cross correlation function	0.950	0.792
		Size	0.844	0.805
		Phase shift	0.665	0.780
		Correlation method	0.852	0.792
	Without comfort liner	Cross correlation function	0.950	0.770
		Size	0.888	0.936
		Phase shift	1.0	1.0
		Correlation method	0.947	0.869
Impact2	With comfort liner	Cross correlation function	0.951	0.776
		Size	0.862	0.650
		Phase shift	0.644	0.833
		Correlation method	0.852	0.759
	Without comfort liner	Cross correlation function	0.960	0.858
		Size	0.90	0.831
		Phase shift	0.893	1.0
		Correlation method	0.928	0.887
Impact3	With comfort liner	Cross correlation function	0.975	0.744
		Size	0.891	0.645
		Phase shift	0.943	0.379
		Correlation method	0.946	0.628
	Without comfort liner	Cross correlation function	0.986	0.894
		Size	0.902	0.990
		Phase shift	0.853	0.786
		Correlation method	0.932	0.891

Appendix 3 – Heat Map of BrIC

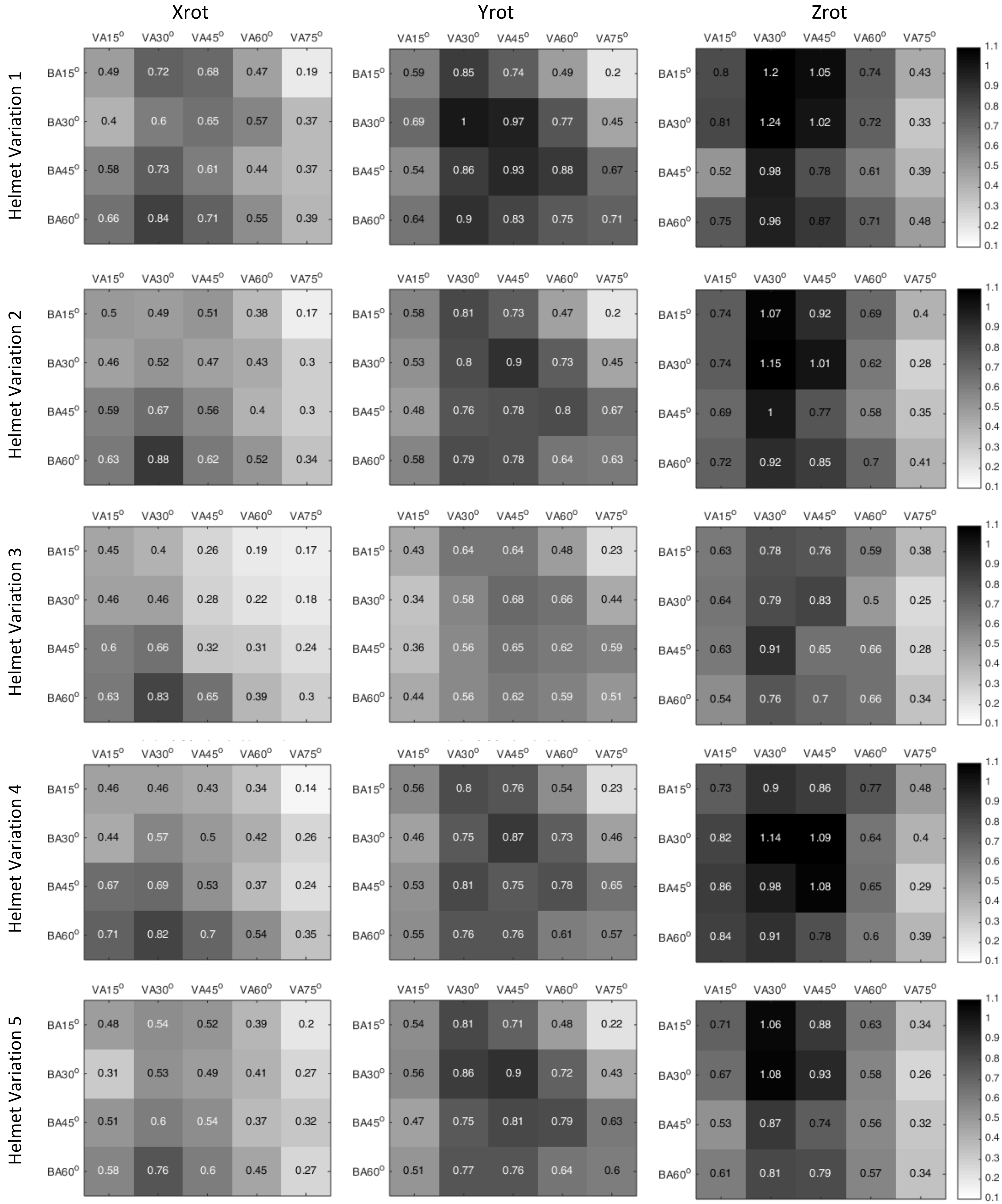

Fig. C1. Heat map shows the numerical value along with the coloUr scale indicating the level of BrIC developed during the helmeted head impact for the entire simulation matrix. The darker colour indicates higher BrIC value, and vice versa.

Appendix 4 – Whole-Body and Head-Only Simulations

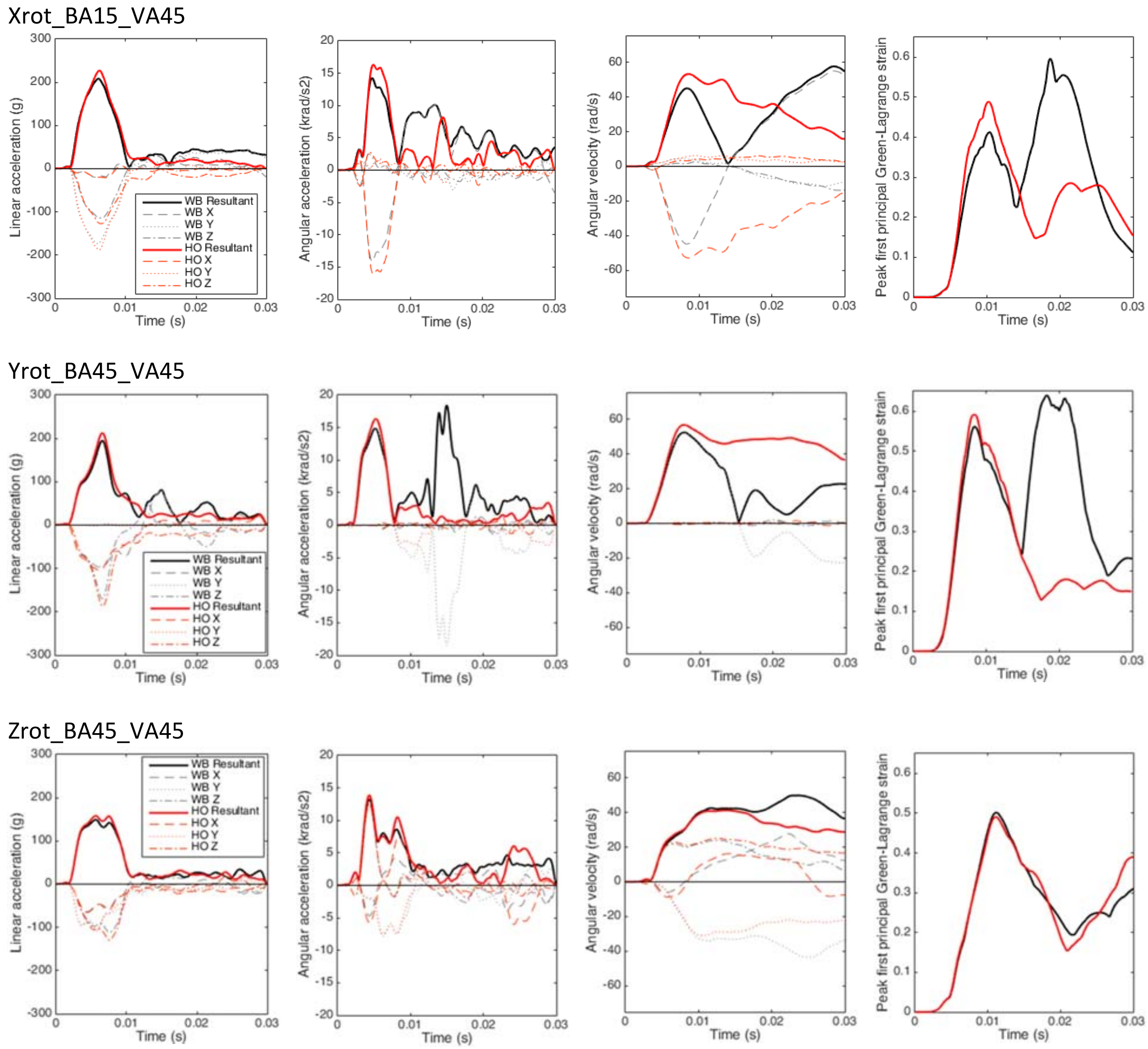

Fig. D1. Head kinematics and/or peak brain strain between head-only (HO) and whole body (WB) simulations. WB/HO X, Y or Y denotes acceleration/velocity around the local head coordinate system. X is in posterior-anterior direction and Z is in inferior-superior direction.